rudzinski@mpip-mainz.mpg.de

Supporting Information for: Dynamical properties across different coarse-grained models for ionic liquids

Joseph F. Rudzinski[1], Sebastian Kloth,[2] Svenja Wörner,[1]
Tamisra Pal,[2] Kurt Kremer,[1], Tristan Bereau,[3,1] Michael Vogel[2]
[1] *Max Planck Institute for Polymer Research, 55128 Mainz, Germany*
[2] *Institute of Condensed Matter Physics, Technische Universität Darmstadt, Hochschulstr. 6, 64289 Darmstadt, Germany and*
[3] *Van 't Hoff Institute for Molecular Sciences and Informatics Institute, University of Amsterdam, Amsterdam 1098 XH, The Netherlands*
(Dated: February 2, 2021)

I. COMPUTATIONAL METHODS: ADDITIONAL DETAILS

A. Parametrization of the thermo* model

As described in the Methods section of the main text, the thermo* model is a refinement of the thermo model, determined by applying the iter-gYBG approach to each of the short-ranged nonbonded interactions (while keeping all other interactions fixed), but restricting the calculation to relatively short distances between CG sites. In particular, the change in the force coefficients were calculated up to the distance corresponding to the minimum of each of the potentials. Table S3 presents this cut-off distance used for each pair type.

TABLE S1. Cut-off values for parametrization of the thermo* model.

Pair Type	r_{cut} [nm]
I1-I1	0.469
I1-I2	0.464
I1-I3	0.464
I1-CT	0.497
I1-PF	0.584
I2-I2	0.469
I2-I3	0.464
I2-CT	0.497
I2-PF	0.584
I3-I3	0.412
I3-CT	0.435
I3-PF	0.555
CT-CT	0.525
CT-PF	0.566
PF-PF	0.595

B. Calculation of thermodynamic properties

Density: To determine the equilibrium density of the thermo* model, we performed a 25 ns simulation in the NPT ensemble with $T = 300\,\mathrm{K}$ and $P = 1\,\mathrm{bar}$. Similar to the NVT simulations described in the main text, these simulations used the stochastic dynamics integrator with a temperature coupling constant of 2 ps, a 1 fs time step, and periodic boundary conditions. For pressure coupling, the Parrinello-Rahman barostat [1] was employed with a coupling constant of 10 ps and compressibility of $4.5 \cdot 10^{-5}\,\mathrm{bar}^{-1}$.

TABLE S2. Equilibrium densities at 1 bar. Experimental densities from [2].

Temp [K]	ρ [g/cm^3]		
	Expt	AA	thermo
260	1.404	1.428	1.390
270	1.395	1.415	1.382
280	1.387	1.403	1.374
300	1.369	1.389	1.357
320	1.352	1.363	1.337
350	1.326	1.333	1.313
400	1.282	1.273	1.269

Surface tension: To determine the surface tension of the thermo* model, we performed "slab" simulations that probe the vacuum-water interface. More specifically, starting from 9 independent configurations from the production NVT simulations (sampled 1 ns apart), we extended the box length in the z direction to 9 nm. We then performed a 10 ns simulation for each of them using the same parameters as described in the main text, and calculated the surface tension, γ, according to [3, 4]:

$$\gamma = -L_z/4 \cdot (p_{xx} + p_{yy} - 2p_{zz})\,, \tag{S1}$$

where p_{xx}, p_{yy}, and $2p_{zz}$ are the diagonal elements of the pressure tensor and L_z is the box length in z direction. The reported surface tension for the model was determined by averaging this result over the nine independent simulations.

C. Experimental dynamics

TABLE S3. Diffusion constants from experimental measurements [2] and the all-atom reference simulations used in this work. Note that the AA simulations for 260, 270, and 280 K are not fully equilibrated and were not used in the main text to assess dynamical quantities.

Ion Type	Temp [K]	D [10^5 nm^2/ps]	
		Expt	AA
Cation	260	0.0292	0.0346
	270	0.0855	0.0903
	280	0.206	0.255
	300	0.802	0.657
	320	2.17	2.01
	350	6.41	5.82
	400	20.9	24.0
Anion	260	0.0199	0.0228
	270	0.0591	0.0628
	280	0.145	0.164
	300	0.586	0.487
	320	1.64	1.52
	350	5.13	4.91
	400	17.9	20.5

[1] M. Parrinello and A. Rahman, J. Appl. Phys. **52**, 7182 (1981).
[2] H. Tokuda, K. Hayamizu, K. Ishii, M. Abu Bin Hasan Susan, and M. Watanabe, J. Phys. Chem. B **108**, 16593 (2004).
[3] J. Lpez-Lemus and J. Alejandre, Molecular Physics **100**, 2983 (2002).
[4] D. Brown and S. Neyertz, Molecular Physics **84**, 577 (1995).

II. SUPPLEMENTARY RESULTS

A. Force fields

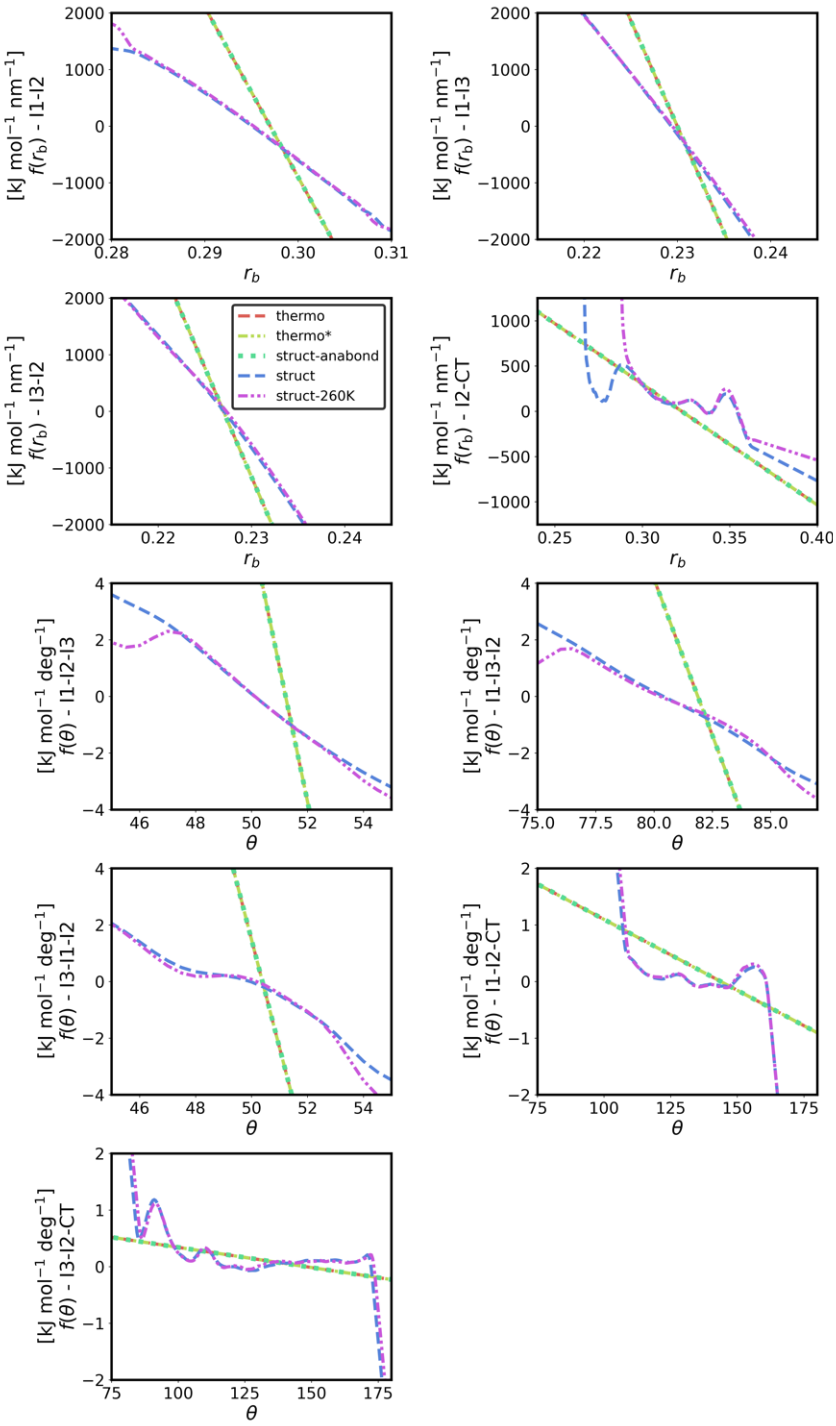

FIG. S1. Comparison of intramolecular force functions for the thermo (red dashed curve), thermo* (yellow dash-dotted curve), struct-anabond (green dotted curve), struct (blue dashed curve), and struct-260K (purple dash-dotted curve) models.

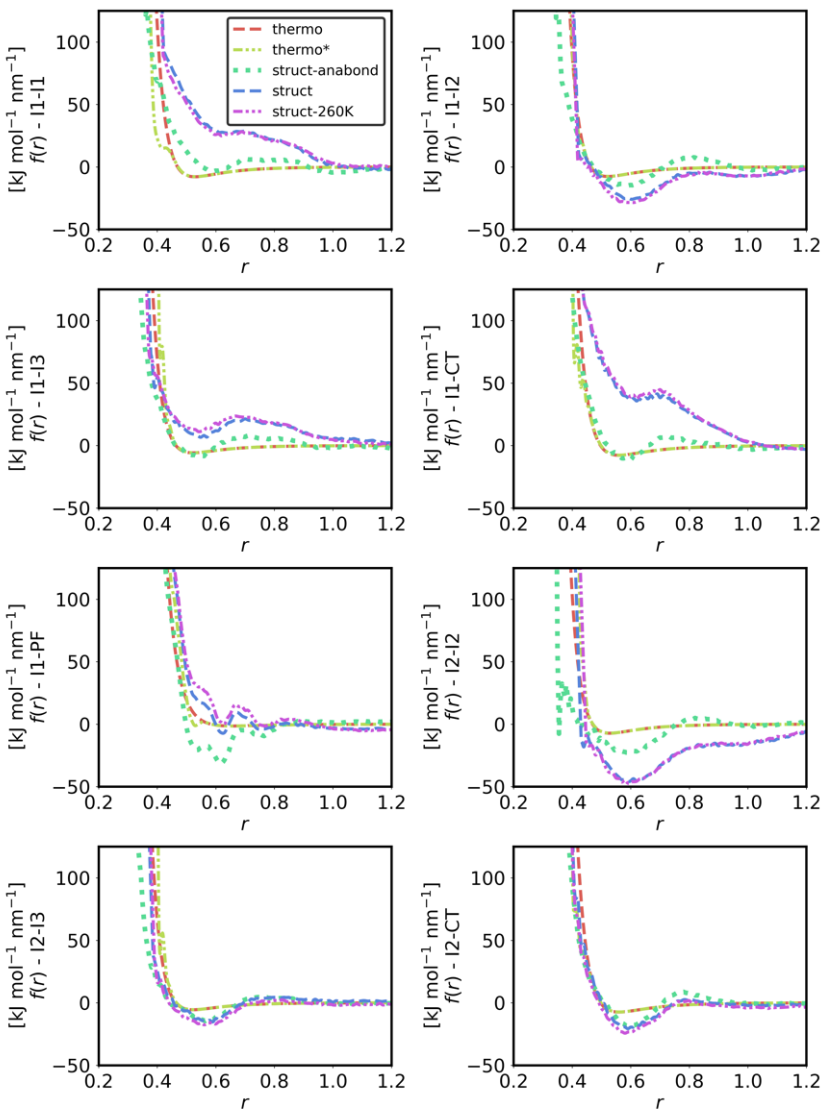

FIG. S2. Comparison of intermolecular force functions for the thermo (red dashed curve), thermo* (yellow dash-dotted curve), struct-anabond (green dotted curve), struct (blue dashed curve), and struct-260K (purple dash-dotted curve) models.

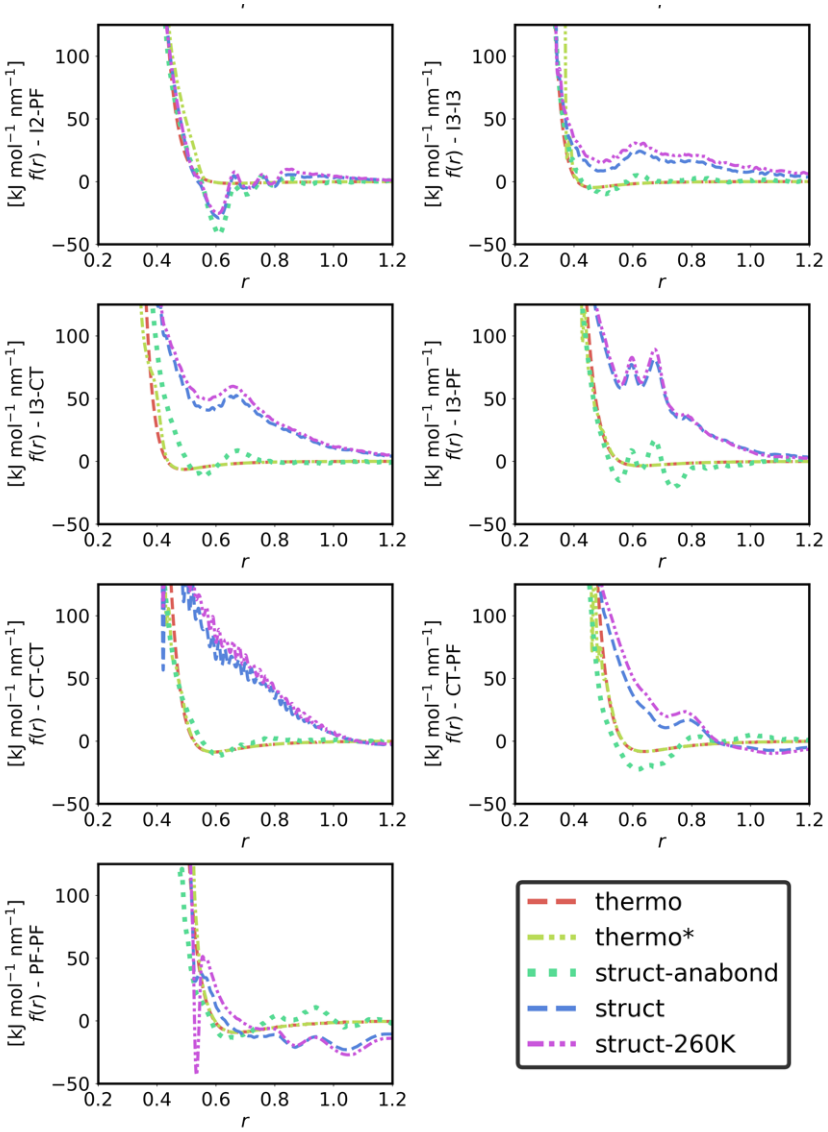

FIG. S3. Comparison of intermolecular force functions for the thermo (red dashed curve), thermo* (yellow dash-dotted curve), struct-anabond (green dotted curve), struct (blue dashed curve), and struct-260K (purple dash-dotted curve) models.

B. 1-D distributions at 300 K

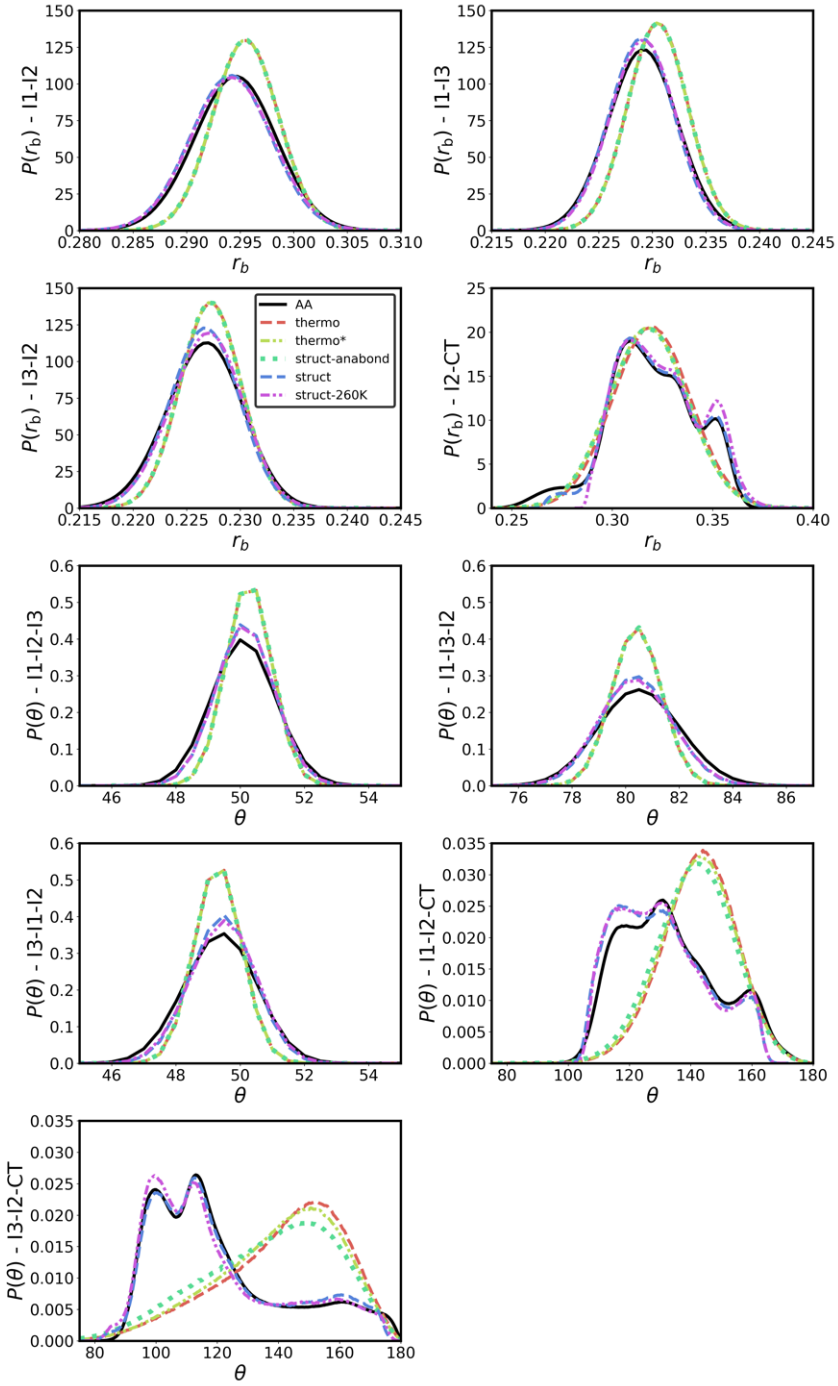

FIG. S4. Comparison of intramolecular 1-D distributions at 300 K for the AA (black solid curve), thermo (red dashed curve), thermo* (yellow dash-dotted curve), struct-anabond (green dotted curve), struct (blue dashed curve), and struct-260K (purple dash-dotted curve) models.

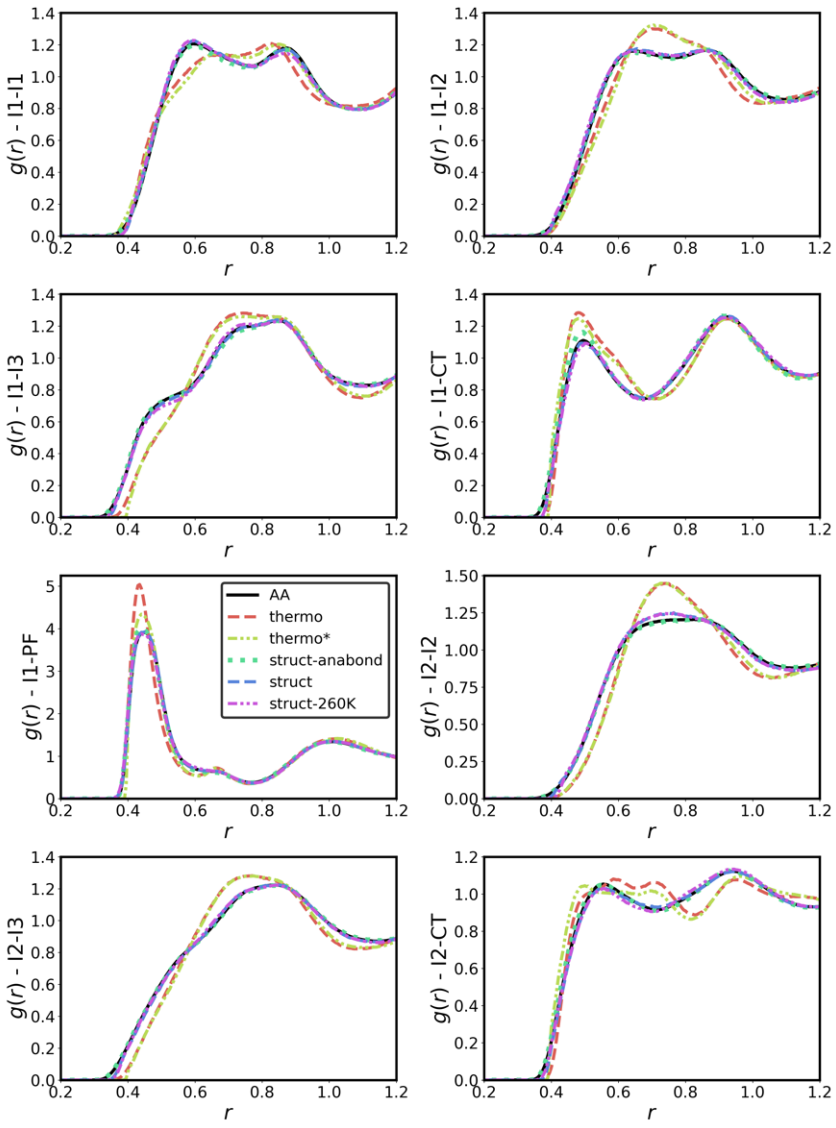

FIG. S5. Comparison of intermolecular 1-D distributions at 300 K for the AA (black solid curve), thermo (red dashed curve), thermo* (yellow dash-dotted curve), struct-anabond (green dotted curve), struct (blue dashed curve), and struct-260K (purple dash-dotted curve) models.

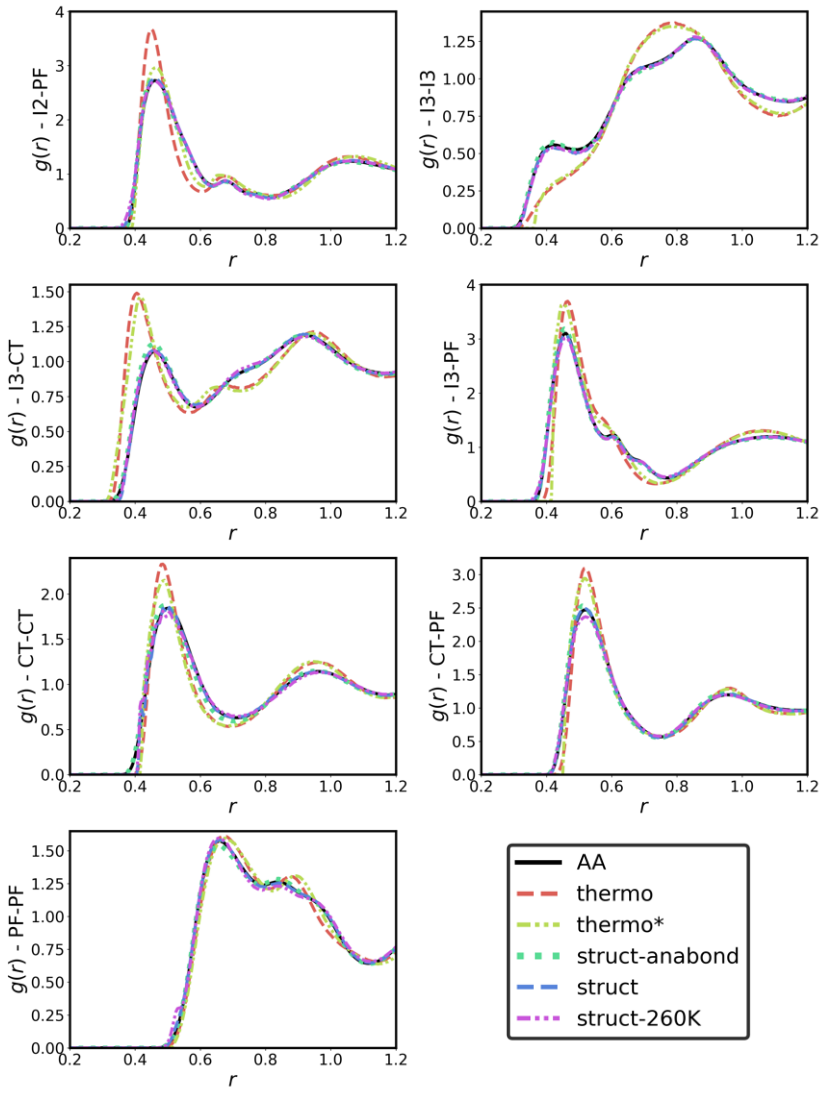

FIG. S6. Comparison of intermolecular 1-D distributions at 300 K for the AA (black solid curve), thermo (red dashed curve), thermo* (yellow dash-dotted curve), struct-anabond (green dotted curve), struct (blue dashed curve), and struct-260K (purple dash-dotted curve) models.

C. Temperature dependence of 1-D distributions

1. *AA model*

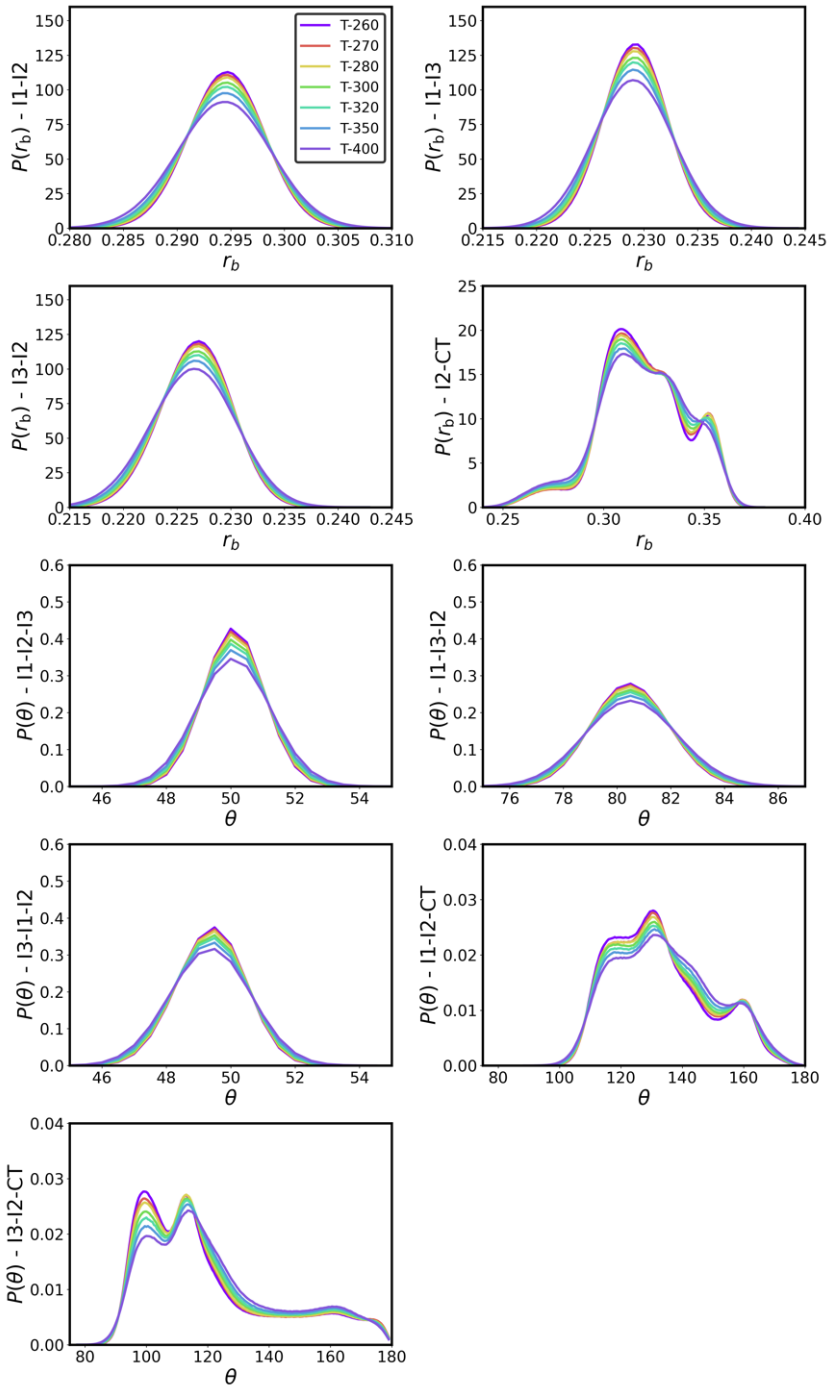

FIG. S7. Temperature dependence of the intramolecular 1-D distributions for the AA model.

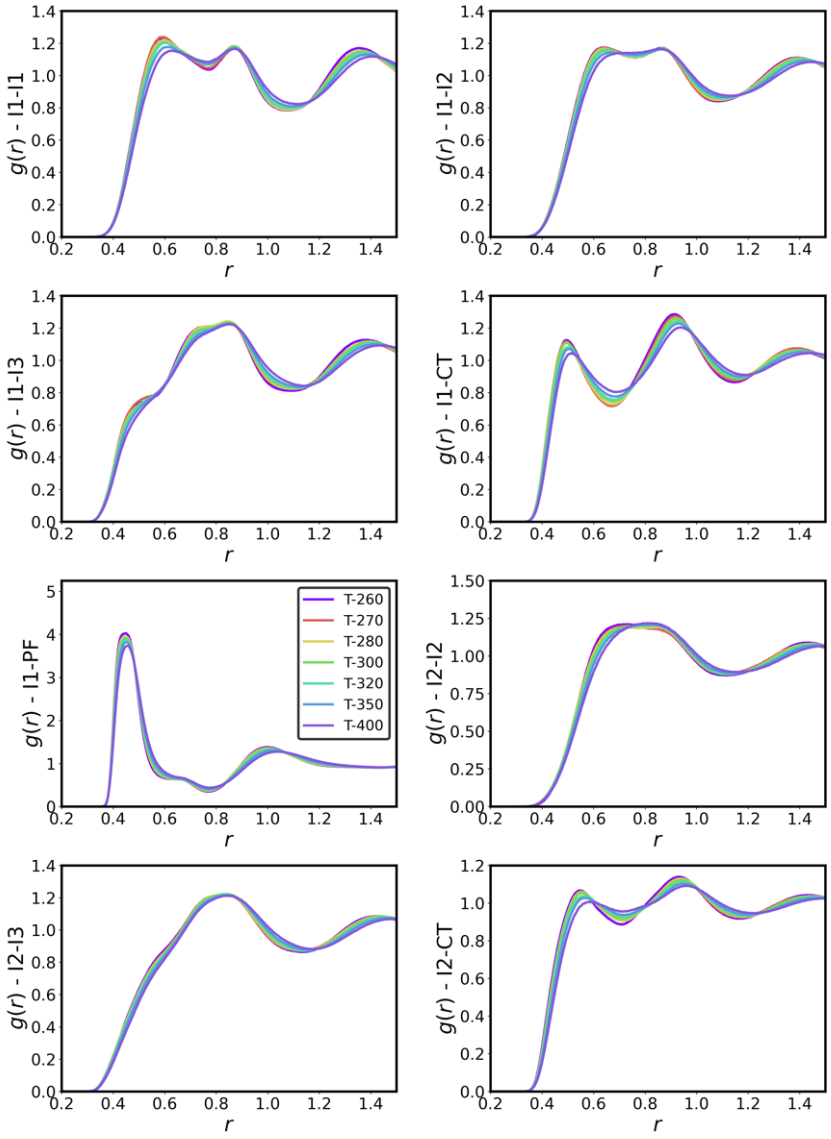

FIG. S8. Temperature dependence of the intermolecular 1-D distributions for the AA model.

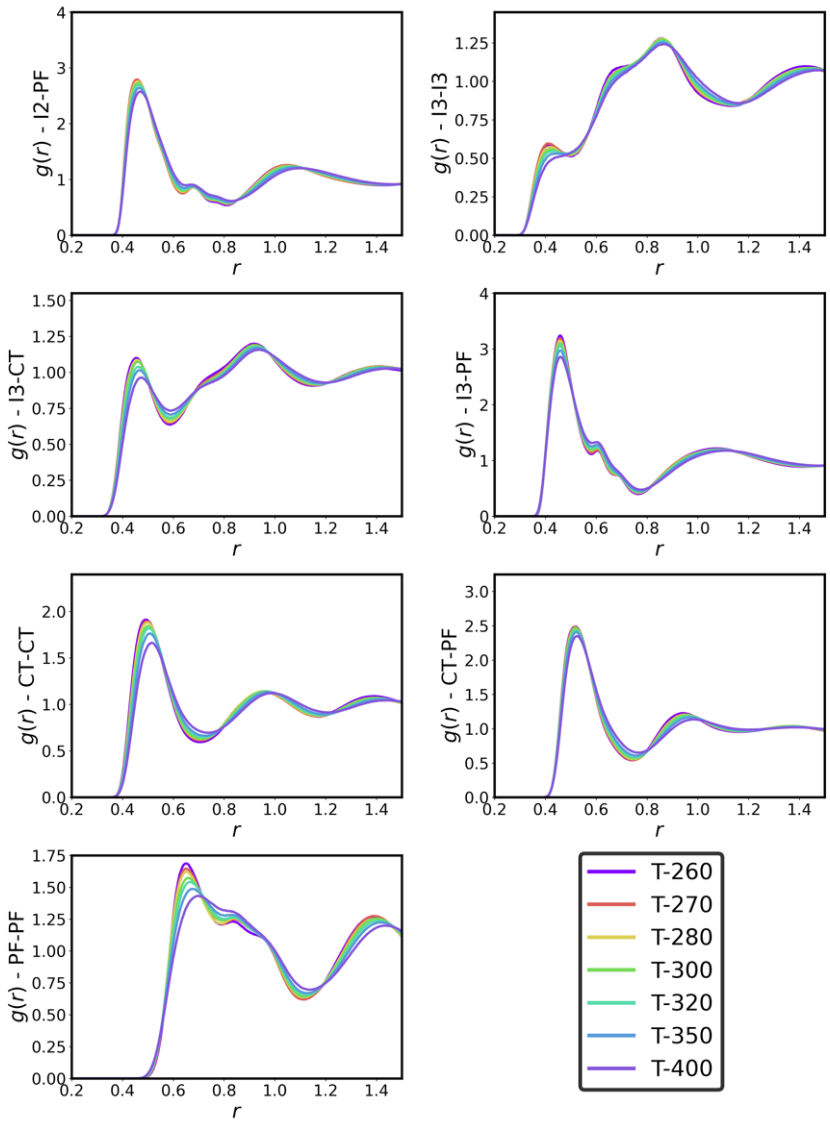

FIG. S9. Temperature dependence of the intermolecular 1-D distributions for the AA model.

2. thermo model

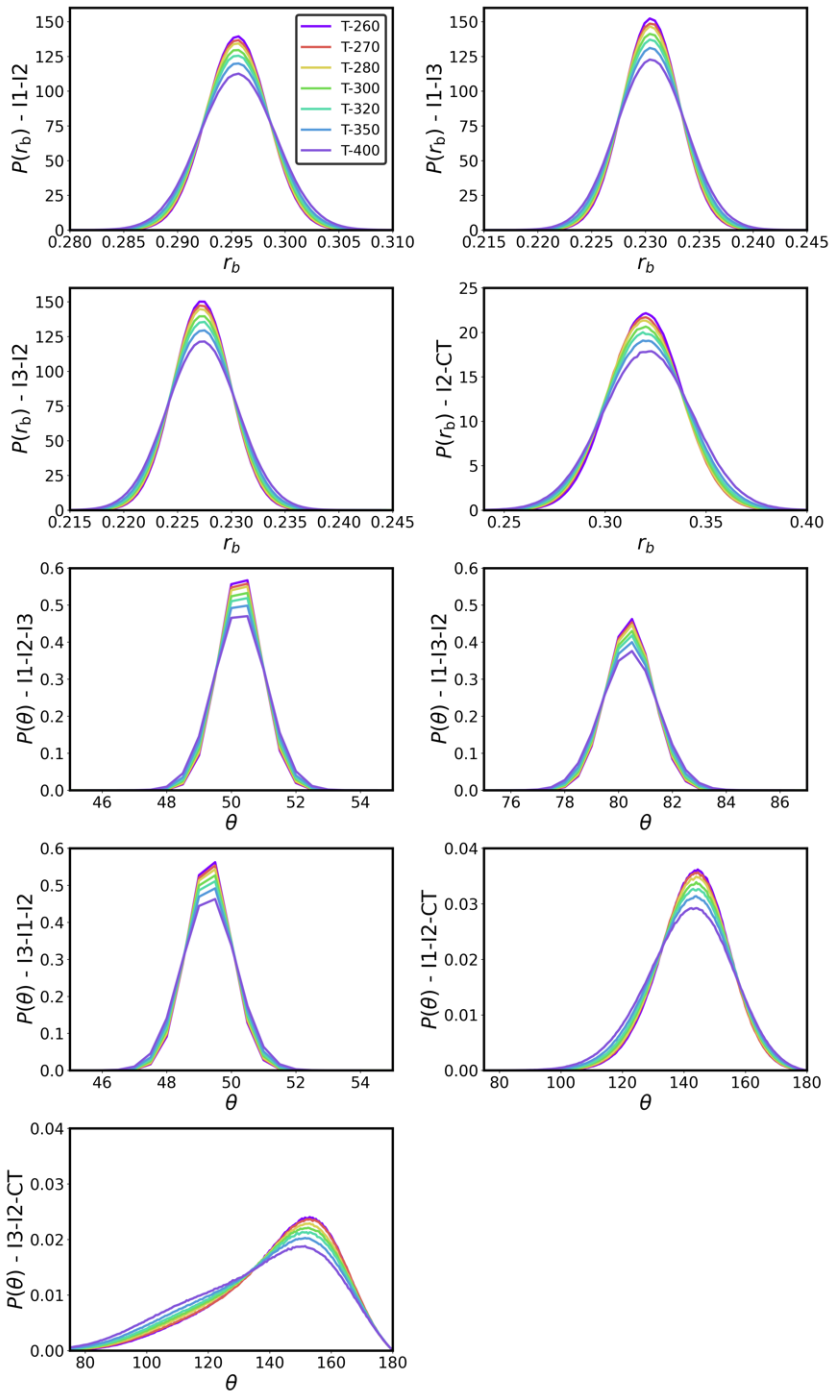

FIG. S10. Temperature dependence of the intramolecular 1-D distributions for the thermo model.

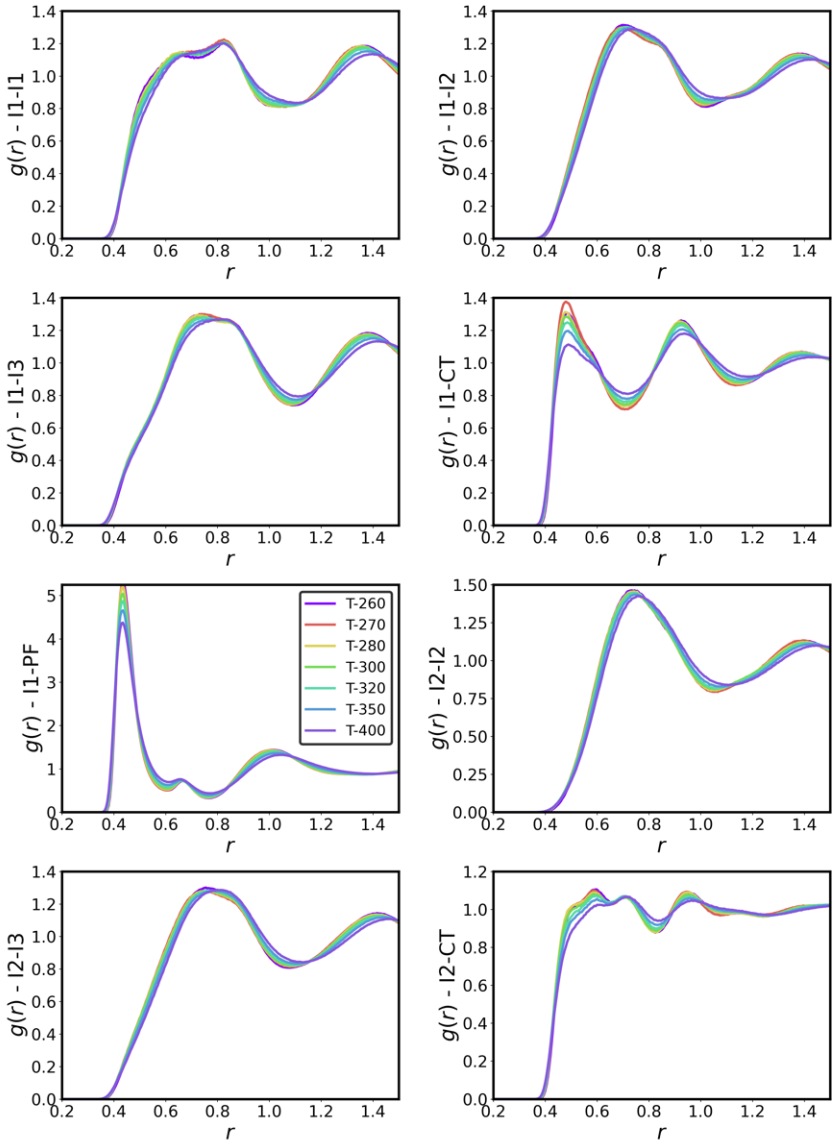

FIG. S11. Temperature dependence of the intermolecular 1-D distributions for the thermo model.

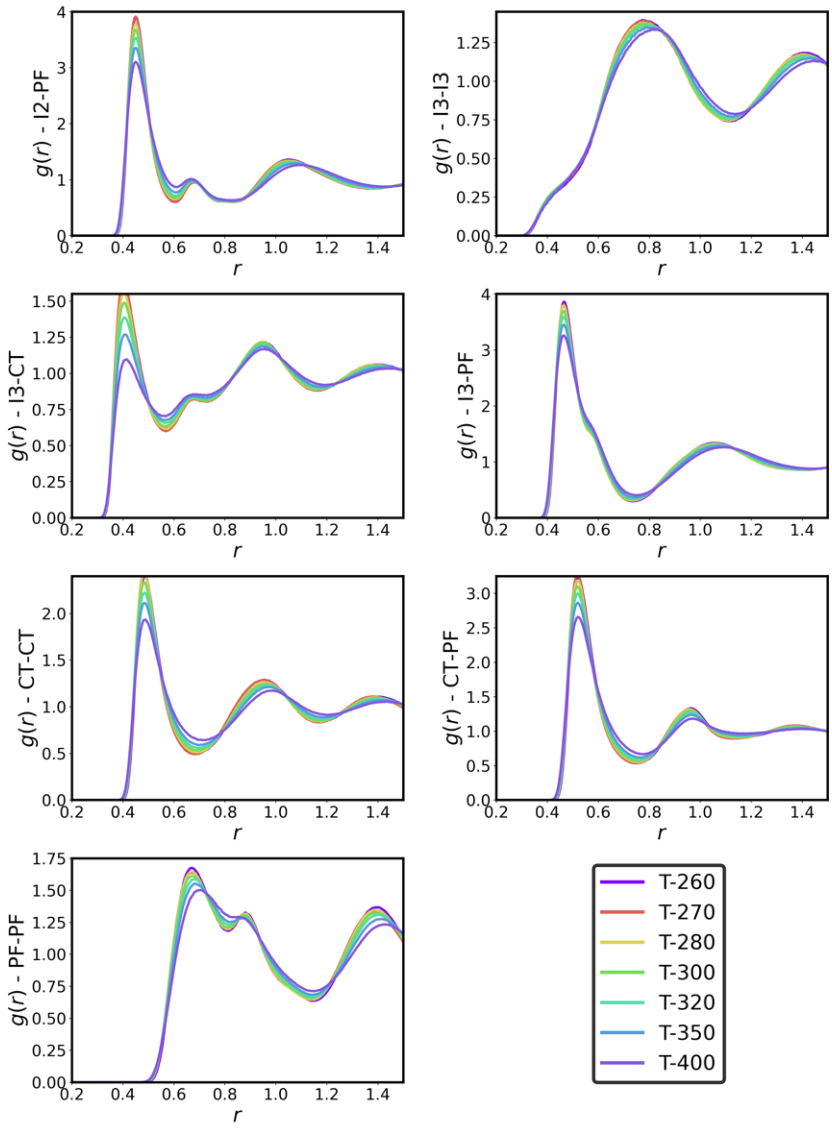

FIG. S12. Temperature dependence of the intermolecular 1-D distributions for the thermo model.

3. *thermo* model*

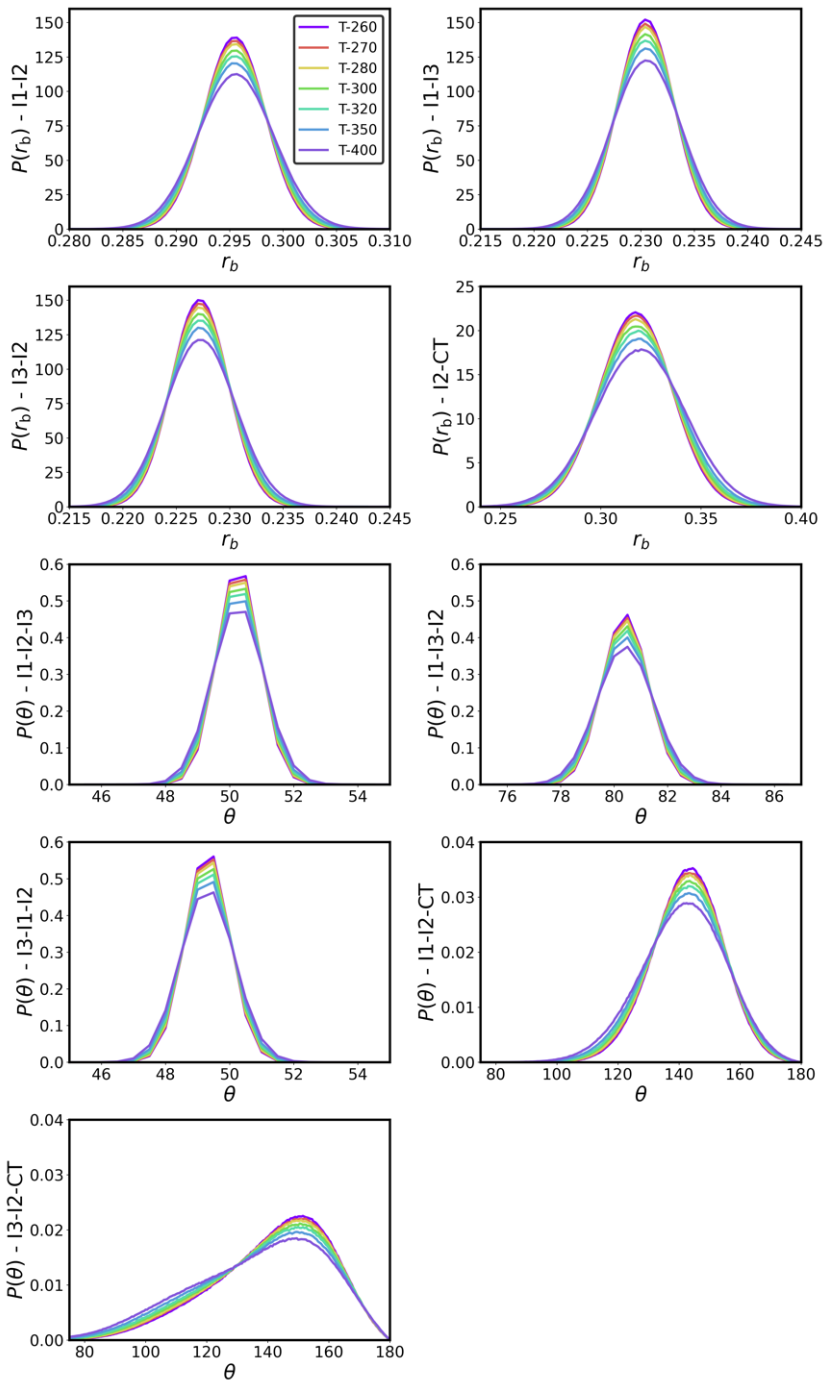

FIG. S13. Temperature dependence of the intramolecular 1-D distributions for the thermo* model.

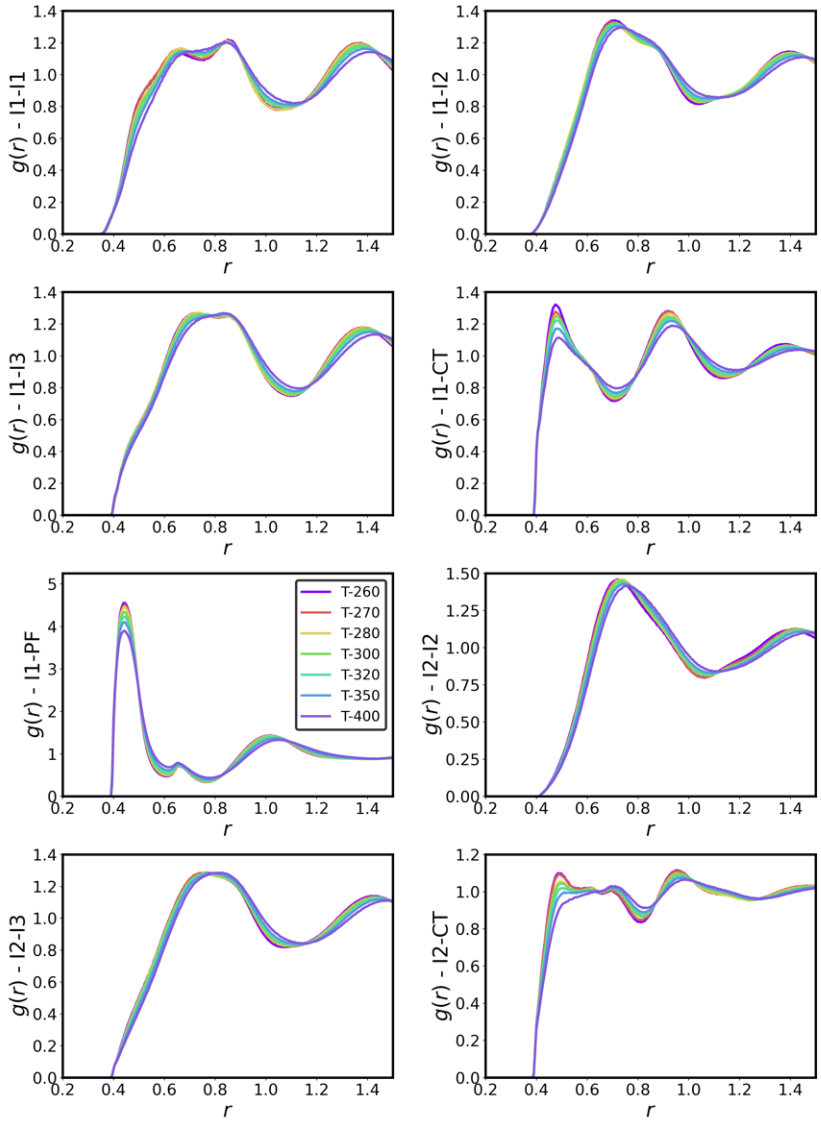

FIG. S14. Temperature dependence of the intermolecular 1-D distributions for the thermo* model.

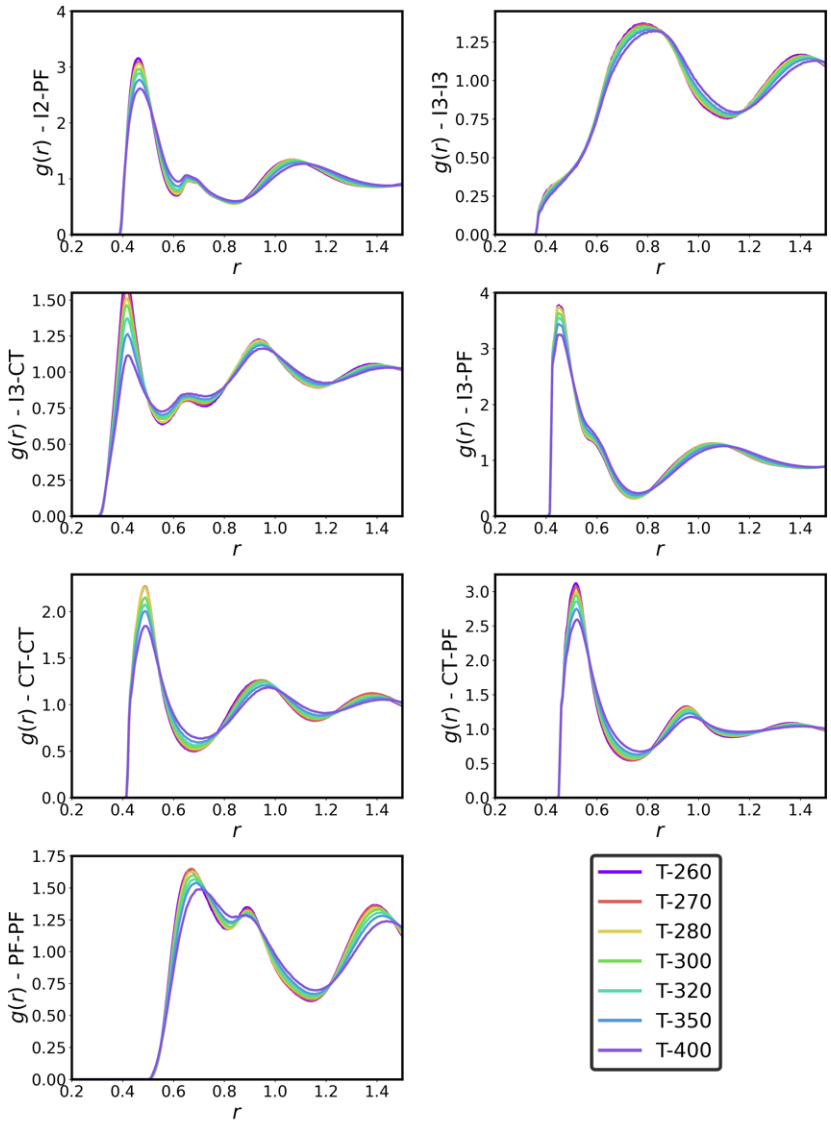

FIG. S15. Temperature dependence of the intermolecular 1-D distributions for the thermo* model.

4. struct-anabond model

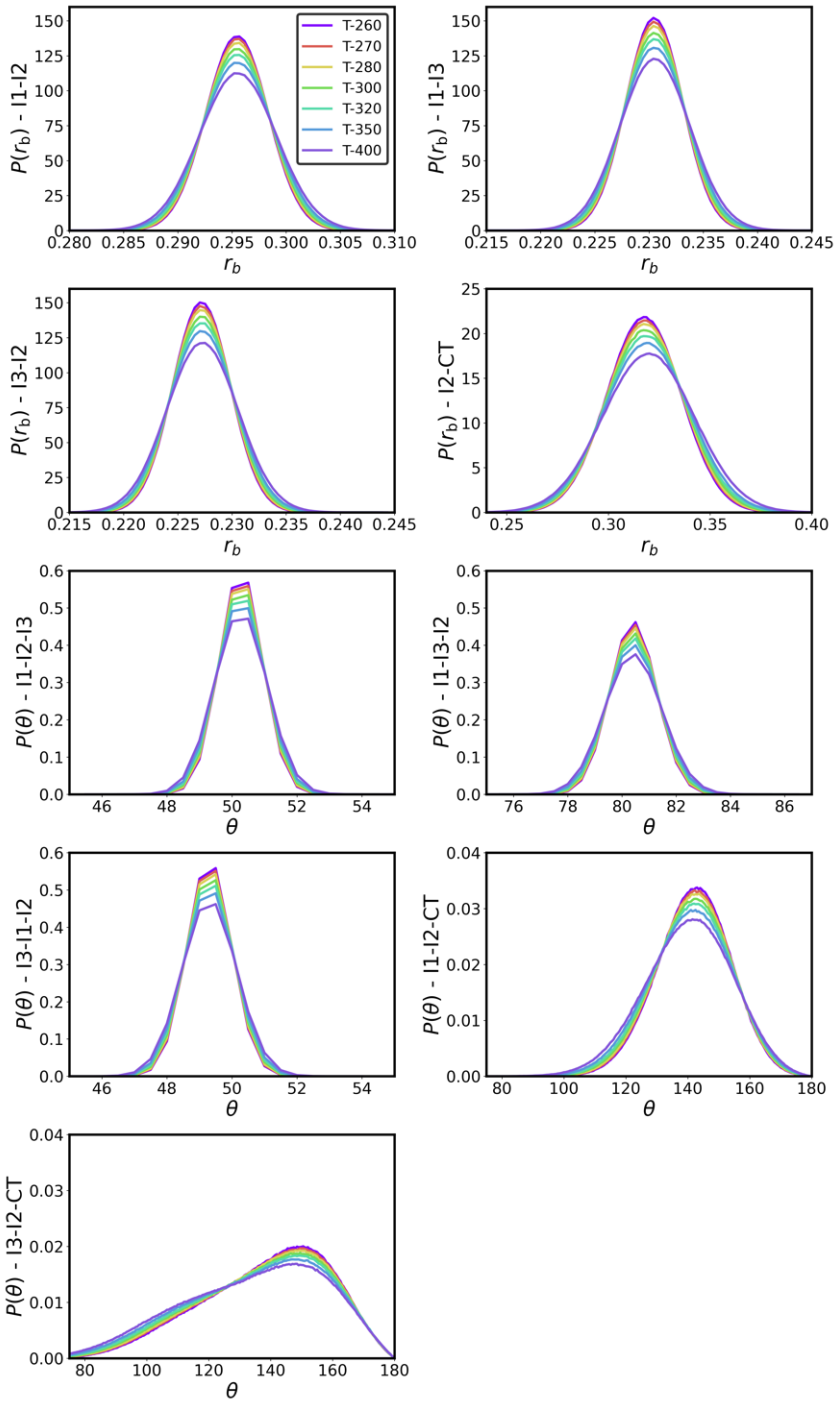

FIG. S16. Temperature dependence of the intramolecular 1-D distributions for the struct-anabond model.

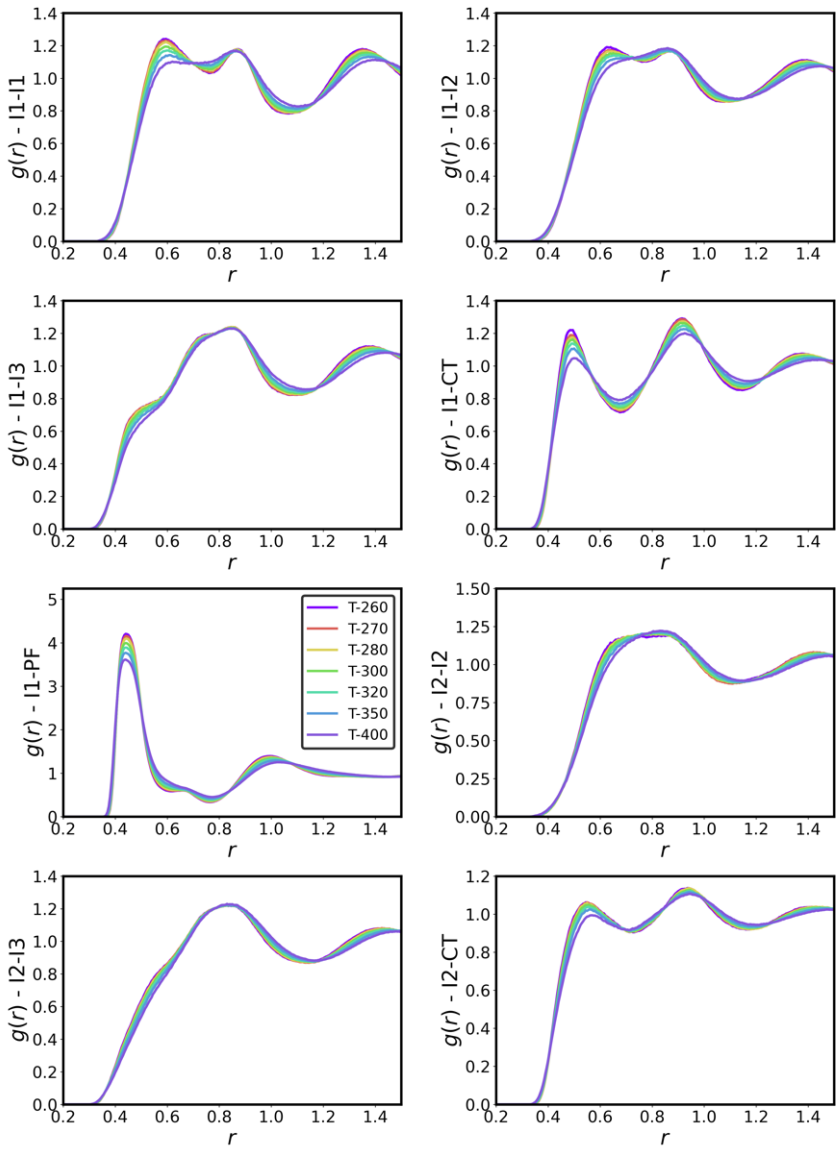

FIG. S17. Temperature dependence of the intermolecular 1-D distributions for the struct-anabond model.

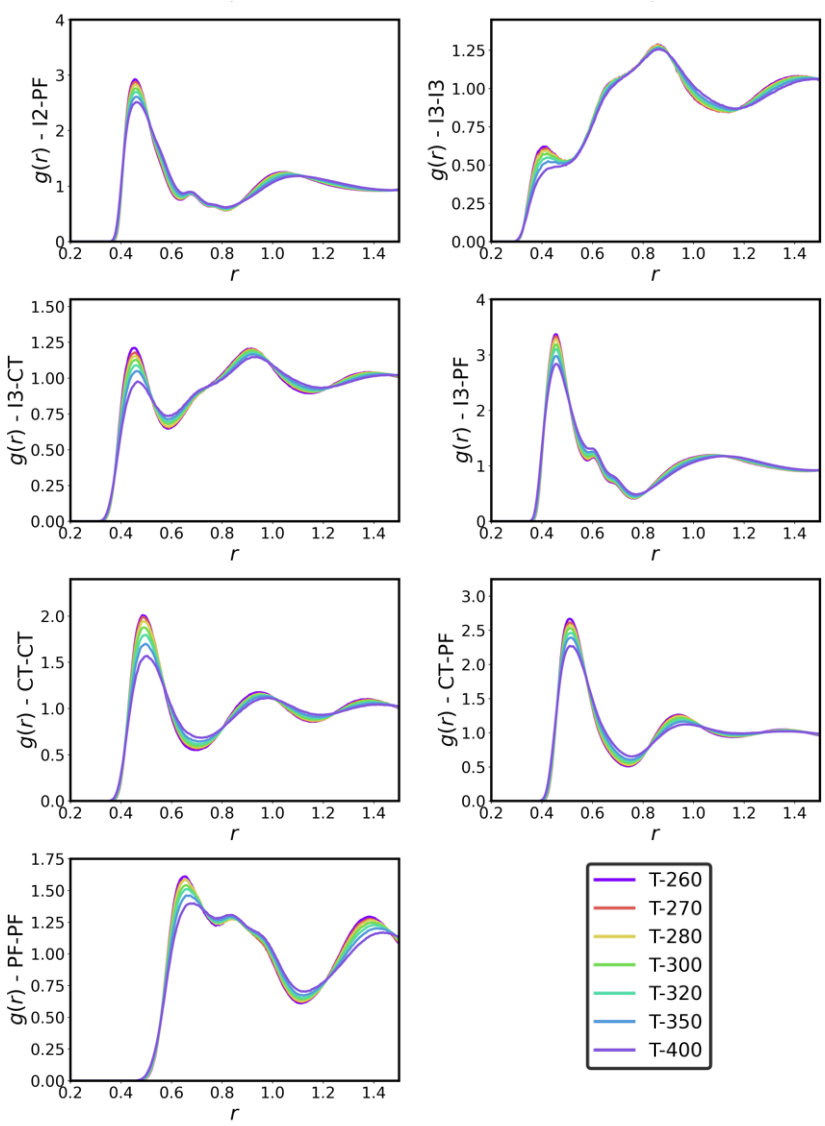

FIG. S18. Temperature dependence of the intermolecular 1-D distributions for the struct-anabond model.

5. struct model

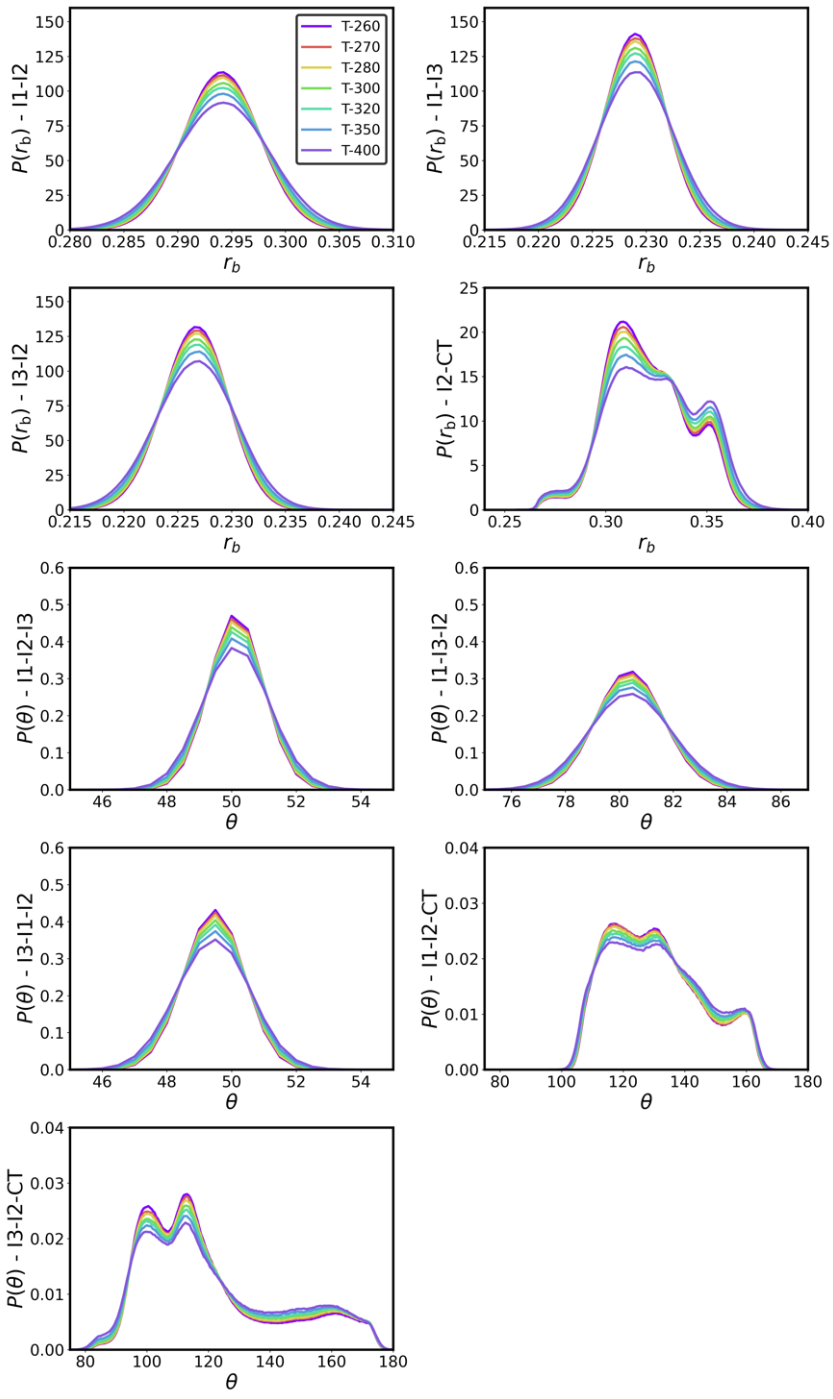

FIG. S19. Temperature dependence of the intramolecular 1-D distributions for the struct model.

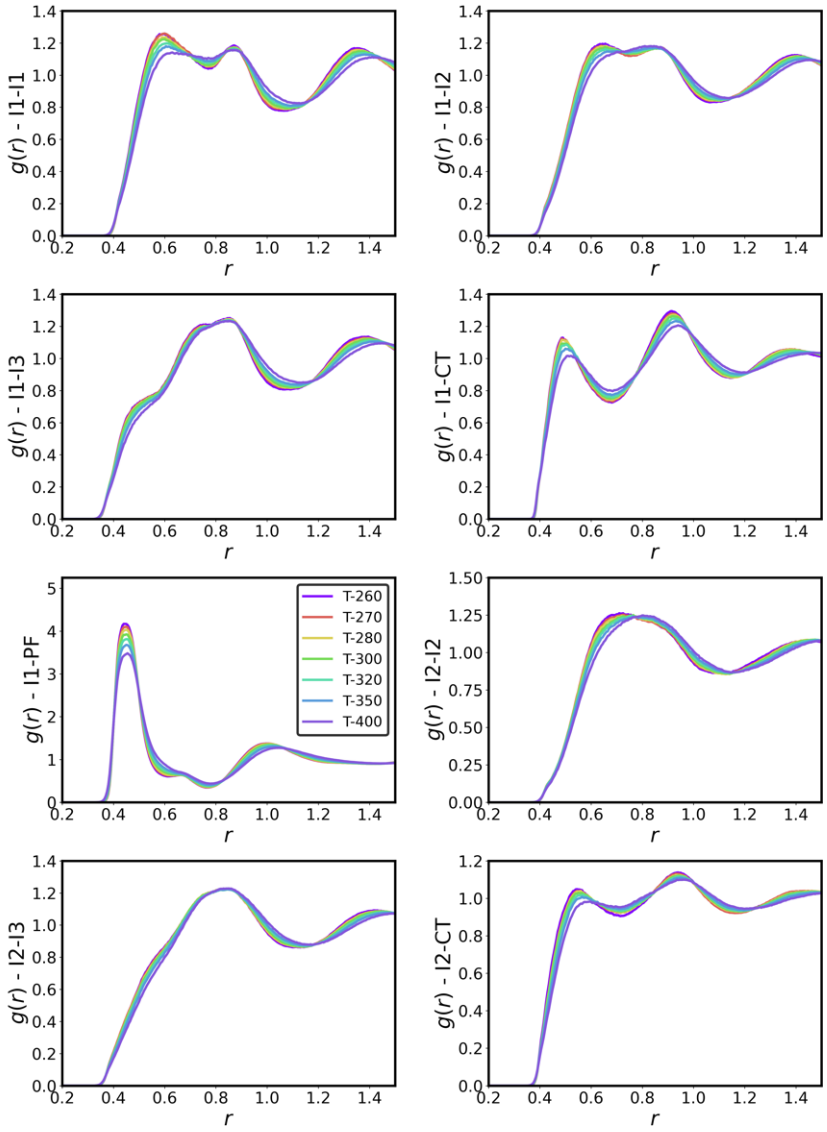

FIG. S20. Temperature dependence of the intermolecular 1-D distributions for the struct model.

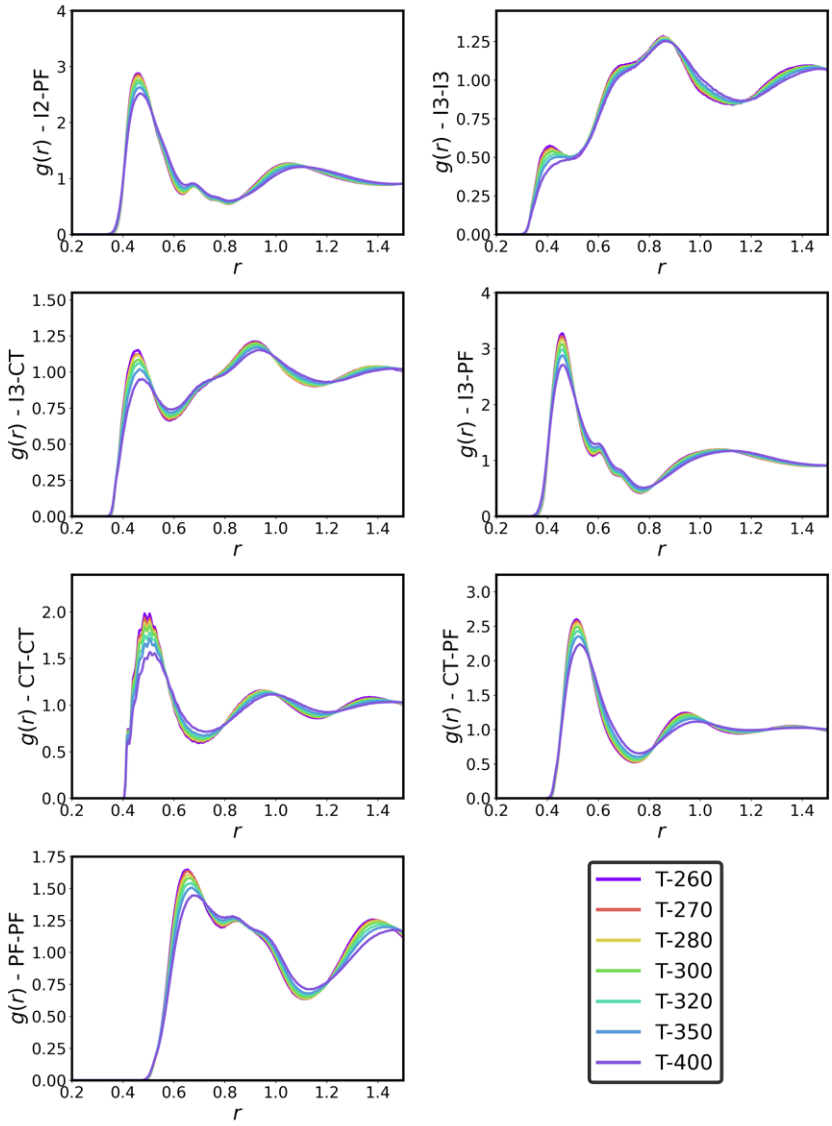

FIG. S21. Temperature dependence of the intermolecular 1-D distributions for the struct model.

6. struct-260K

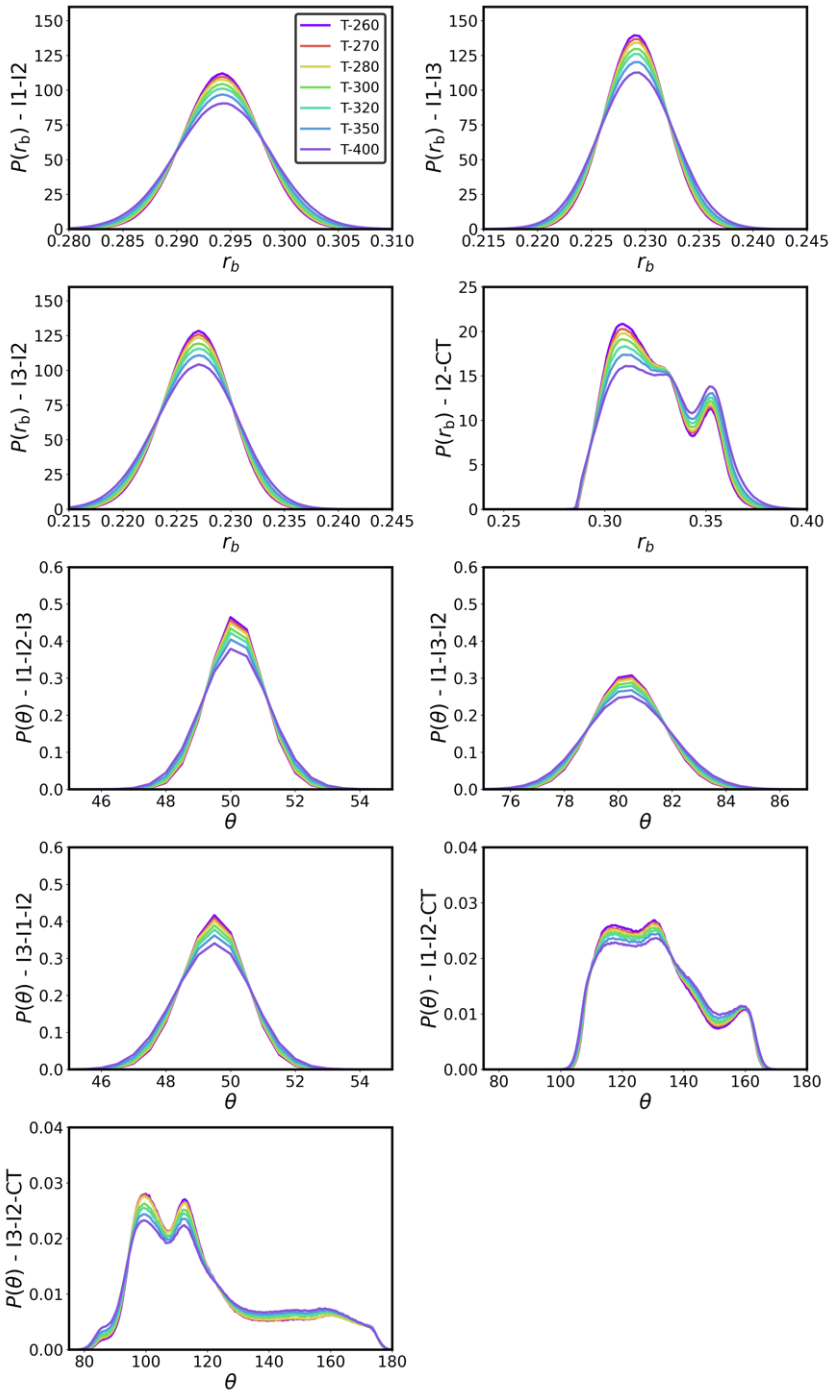

FIG. S22. Temperature dependence of the intramolecular 1-D distributions for the struct-260K model.

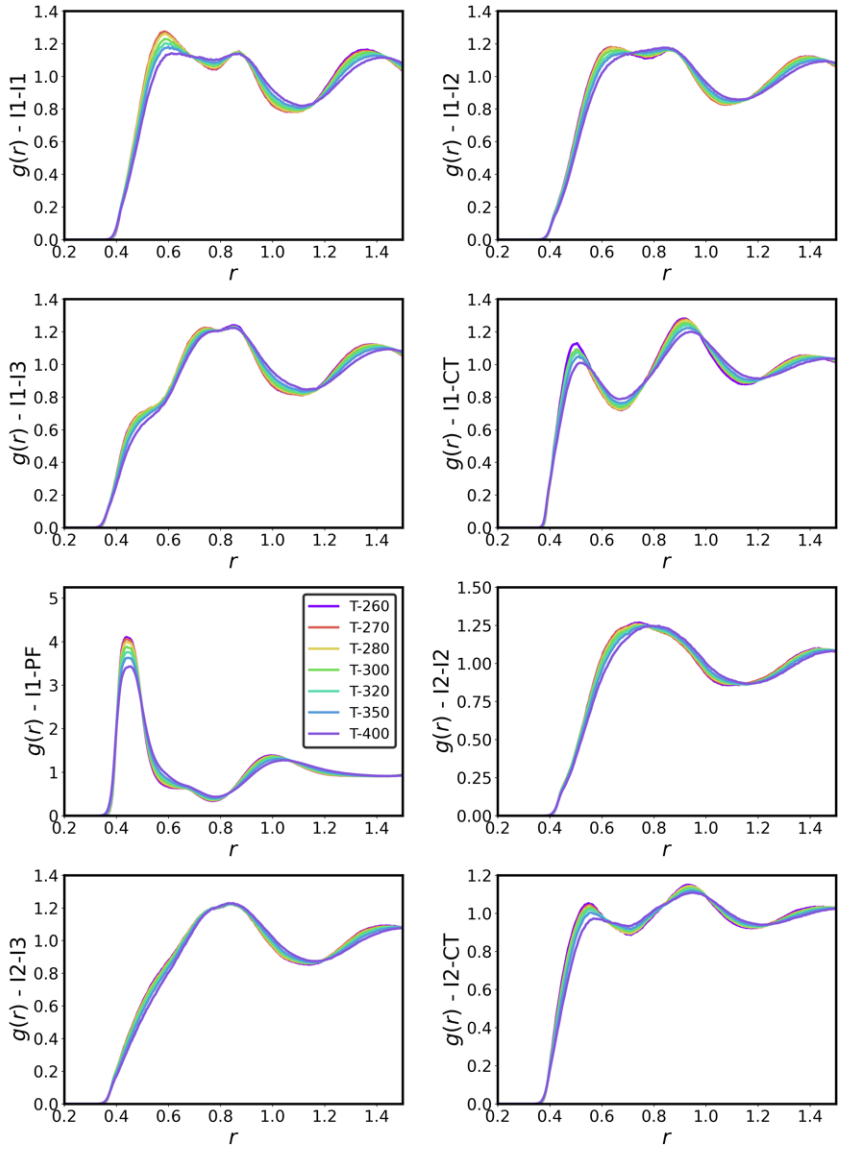

FIG. S23. Temperature dependence of the intermolecular 1-D distributions for the struct-260K model.

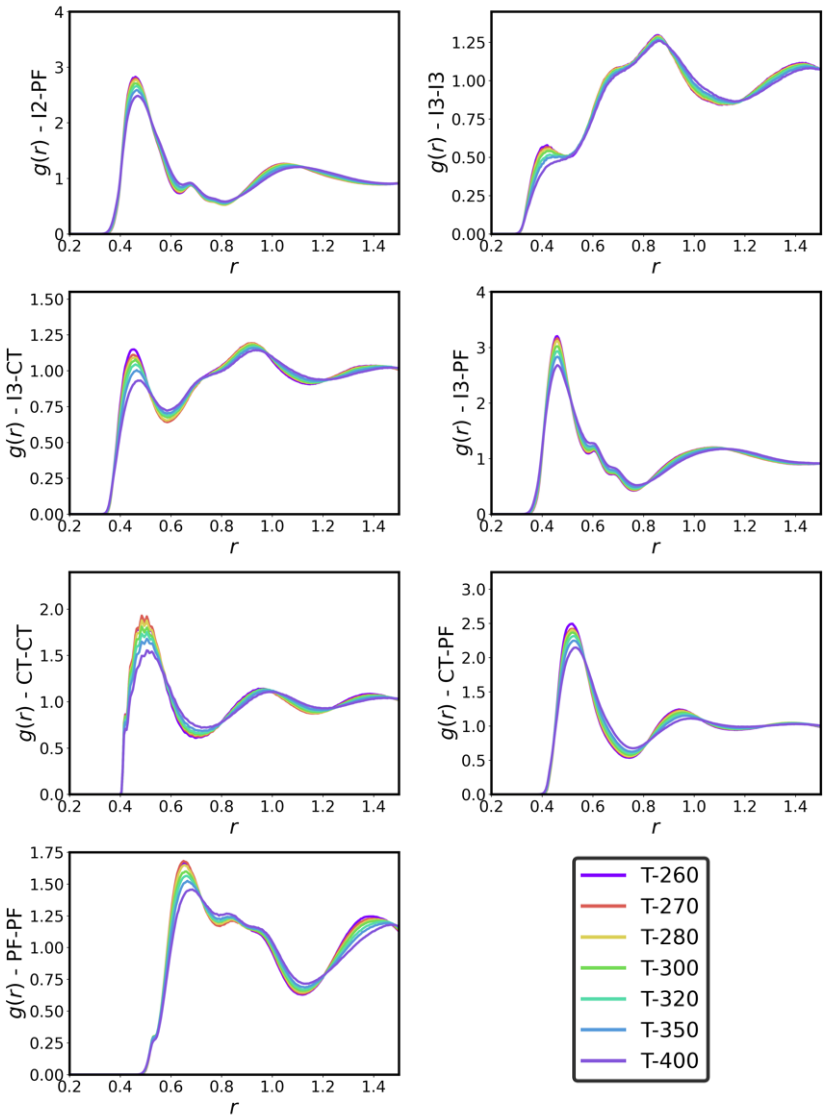

FIG. S24. Temperature dependence of the intermolecular 1-D distributions for the struct-260K model.

D. Dynamical properties

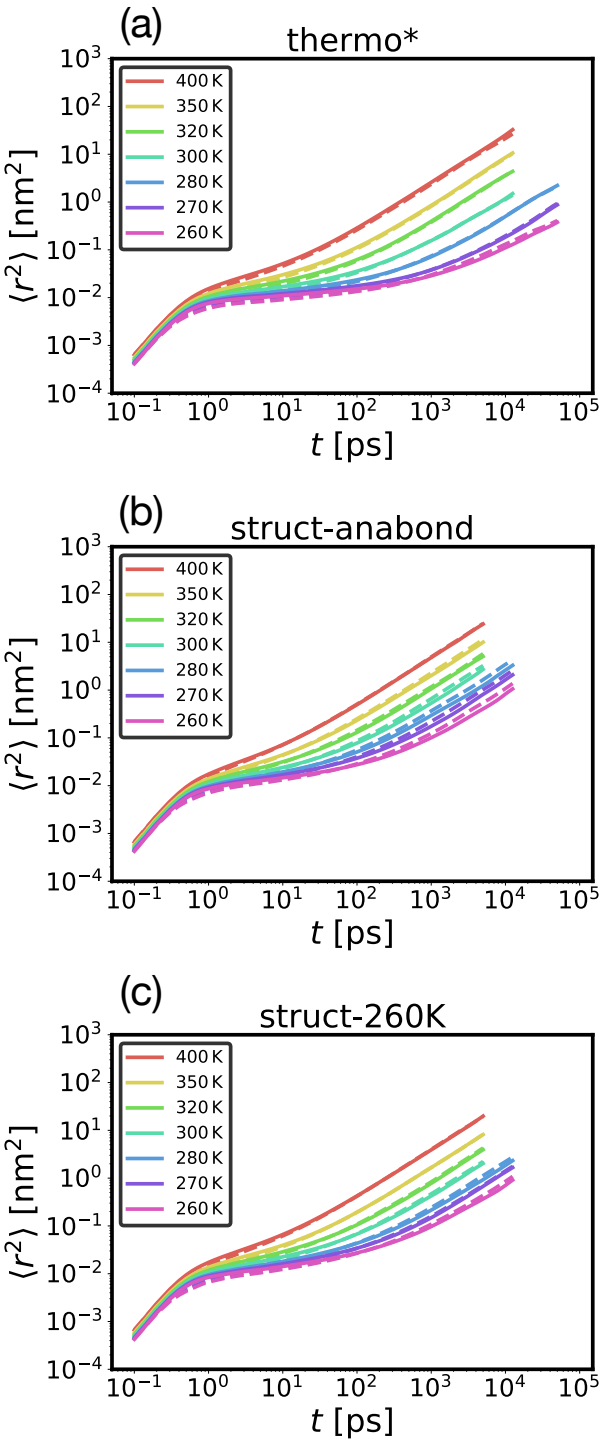

FIG. S25. Mean squared displacement (MSD), $\langle r^2 \rangle$, as a function of time for the (a) thermo*, (b) struct-anabond, and (c) struct-260K models.